Phase formation features during metallothermic reduction of natural wolframite

K. V. Pikulin, *Candidate of Technical Sciences, Senior Researcher*[1], *pikulin.imet@gmail.com*
L. I. Galkova, *Candidate of Technical Sciences, Senior Researcher*[1]
R. I. Gulyaeva, *Candidate of Chemical Sciences, Senior Researcher*[1]
L. Yu. Udoeva, *Candidate of Technical Sciences, Leading Researcher*[1]
S. V. Sergeeva, *Candidate of Technical Sciences, Senior Researcher*[1]
S. N. Tyushnyakov, *Candidate of Technical Sciences, Leading Researcher*[1]

[1]*Vatolin Institute of Metallurgy of the Ural Branch of the Russian Academy of Sciences (Ekaterinburg, Russia).*

The phase formation mechanisms during the metallothermic reduction of natural wolframite from the Akchatau Deposit using aluminum and a calcium-aluminum master alloy was investigated in this study. Thermodynamic simulation demonstrates that, regardless of the reducing agent employed (Al or Ca – Al master alloy), the equilibrium composition of the metallic phase consists of tungsten and ferrotungsten. The application of the Ca – Al master alloy increases the thermal effect of the process by 4.3% and raises the adiabatic temperature by 390 °C compared to the conventional aluminothermic route, while also enhancing the separation of the metallic and oxide phases due to the formation of low-melting calcium aluminates. Using differential scanning calorimetry (DSC), *X*-ray diffraction (XRD), and *X*-ray microanalysis (EPMA), it was established that both processes proceed in a stepwise manner; however, their underlying mechanisms differ fundamentally. In the aluminothermic process, the iron-bearing component of the mineral is reduced first, yielding aluminum-based intermetallic compounds, which subsequently react with the manganese-enriched residual wolframite fraction. When the Ca – Al master alloy is employed, the initial stage involves the formation of calcium tungstates ($CaWO_4$, Ca_3WO_6, Ca_2WMnO_6) and aluminides of the principal metals; these intermediates, together with calcium vapor, subsequently reduce the complex oxides formed in the preceding step. It is shown that, in both cases, the final products of natural wolframite reduction are metallic tungsten and its solid solutions with iron and manganese. The results obtained may contribute to the optimization of out-of-furnace metallothermic processing technologies for tungsten-containing raw materials.

Key words: wolframite, metallothermy, aluminum, calcium-aluminum master alloy, phase formation.
DOI: 10.17580/nfm.2026.01.02

Introduction

Tungsten and its alloys are widely used in modern engineering due to their unique combination of properties, including high refractoriness, strength, and wear resistance [1–3]. A significant portion of the tungsten produced and imported in Russia is consumed in the manufacture of ferrotungsten [4], which serves as an alloying additive for steels that undergo further machining [5, 6]. In industrial practice, ferrotungsten is obtained predominantly by carbothermic reduction or metallothermic methods [7, 8]. Metallothermic processes are characterized by high exothermicity, simplicity of equipment design, and the ability to produce alloys with low carbon content and minimal non-metallic impurities, offering economic and technological advantages over carbothermic routes [9, 10]. The primary raw materials for tungsten production are scheelite and wolframite concentrates, with the latter accounting for approximately 50% of processed feedstocks [11]. Scheelite is a calcium tungstate ($CaWO_4$), whereas wolframite represents an isomorphous series of solid solutions of iron and manganese tungstates, $(Fe,Mn)WO_4$ [12].

Among metal reducing agents, aluminum is the most widely used. The use of alternative reductants (Ca, Mg, Si) is largely confined to processes for producing tungsten powders, in which these elements participate predominantly in the vapor phase [13–17]. Despite the extensive industrial application of aluminothermic reduction, the fundamental principles and specific mechanisms underlying the metallothermic reduction of wolframite concentrates remain insufficiently understood. Available literature data are primarily of an applied nature, while fundamental studies have mainly focused on the kinetic analysis of the overall process, without adequately accounting for the specifics of phase evolution or the influence of intermediate oxides on reduction selectivity.

Studies on the reduction of wolframite by aluminum using differential thermal analysis (DTA) have demonstrated [18] that the process proceeds in two stages: within the temperature range of 1000–1300 °C, WO_3 is reduced to metallic tungsten, whereas the reduction of the solid solution (FeO·MnO) is shifted to higher temperatures (1300–1500 °C) and depends on the thermodynamic stability of the solution, which is governed by the FeO/MnO

ratio. The reaction order for WO_3 reduction in wolframites varies from first to second order depending on the initial mineral composition, indicating a complex mechanism controlled by both chemical kinetics and diffusion processes.

In reference [19], the combustion rates of tungsten trioxide mixtures with varying aluminum content were measured for the production of ferrotungsten containing up to 70 wt.% W. It was demonstrated that the mass combustion rate of WO_3 ranges from 17.2 to 17.9 g/(cm^2 · s). The calculated heat release of the process amounts to 2930 kJ/kg, which ensures heating of the reaction products above the melting temperatures of the initial oxides and metals (WO_3, Fe_2O_3, MnO, SiO_2, and Fe) and creates favorable conditions for out-of-furnace production of the target alloy. However, data pertaining to natural tungsten-containing raw materials were not reported in that study.

A promising approach to intensifying the reduction of tungsten trioxide involves the use of complex reducing agents. For instance, the application of nanostructured composites (e.g., Al/Cu) significantly enhances the reactivity of thermite mixtures by increasing the contact area between reactants and lowering the onset temperature of solid-state reactions [20]. However, their use leads to contamination of the alloy with non-ferrous metals, which is unacceptable in the production of ferroalloys. In the WO_3 – C – Al system, the transformation mechanism depends on the aluminum concentration: at low Al content (0.5–1.2 mol per 1 mol WO_3), the process proceeds in multiple stages, whereas with an excess of aluminum (≥1.3 mol), a mechanically activated self-propagating high-temperature synthesis (SHS) is realized, accompanied by substantial heat release and the formation of carbide phases [21].

The efficiency of using a Ca – Al master alloy in the metallothermic processing of rare-metal mineral raw materials containing tantalum and niobium was evaluated previously [22–24]. The higher chemical activity of calcium compared to aluminum enables an increase in the exothermicity of reduction reactions, while its application in the form of a master alloy mitigates issues associated with its instability in air. No data regarding the influence of the Ca – Al master alloy on the phase formation mechanisms and the reduction selectivity of wolframite components were found in the available literature.

The objective of this study is to investigate the phase formation mechanisms during the metallothermic reduction of natural wolframite using both individual aluminum and a Ca – Al master alloy.

Materials and Methods

The material investigated was a monolithic crystal of natural wolframite from the Akchatau Deposit (Kazakhstan), measuring approximately 4 × 4 × 2 cm. According to chemical analysis, the mineral composition (in wt.%) is as follows: 61.1 W, 6.1 Fe, 10.9 Mn, and 0.34 Si. *X*-ray diffraction (XRD) analysis revealed that the initial wolframite consists of two solid solutions of the $Mn_xFe_{1-x}WO_4$ type. Based on previously calculated unit cell parameters [25], their compositions correspond to the formulas $Mn_{0.5}Fe_{0.5}WO_4$ and $Mn_{0.7}Fe_{0.3}WO_4$, with relative abundances of 63.4% and 36.6%, respectively. The structural and phase state of the wolframite sample is described in detail in reference [25].

Prior to the experiments, the wolframite sample was ground to a particle size fraction of –0.1 mm. Aluminum powder (PA4 grade) with a particle size of –0.14 mm and a calcium-aluminum master alloy of eutectic composition (69.4 wt.% Ca) were used as reducing agents. The master alloy was produced by melting aluminum and calcium granules at 900–1000 °C in an inert atmosphere [24]. The alloy consisted of a two-phase mixture of Ca_8Al_3 and $Ca_{13}Al_{14}$. In the experiments, the master alloy was crushed to a particle size fraction of –0.1 mm.

The experimental study of the metallothermic reduction process was carried out using differential scanning calorimetry (DSC) on a Netzsch STA 449 C Jupiter thermal analyzer. The experiments were performed in a continuous heating mode up to 1200 or 1450 °C, followed by cooling to 500 °C. The components were thoroughly mixed in predetermined proportions, placed into a crucible, compacted, and heated at a rate of 20 °C/min under a high-purity argon flow (99.998% Ar, 30 cm^3/min). The mass of the charge samples ranged from 24 to 27 mg.

The phase composition of the mineral reduction products was determined by *X*-ray diffraction (XRD) using a D8 ADVANCE diffractometer (Cu-K_α radiation, VANTEC-1 position-sensitive detector, β-filter). Data were collected over an angular range of 5–105° 2θ with a step size of 0.021° and a counting time of 1500 s per step. Phase identification was performed using the DIFFRAC^{plus}: EVA software package and the ICDD PDF-4 database. The quantitative phase composition was determined by full-profile Rietveld refinement using the TOPAS software.

To investigate the microstructural features of the metallothermic reduction products of wolframite, scanning electron microscopy (SEM) and electron probe microanalysis (EPMA) were employed. Backscattered electron (BSE) images for phase-specific elemental analysis were acquired using a JSM-5900 LV scanning electron microscope equipped with an Oxford INCA Energy 200 energy-dispersive *X*-ray spectrometer, as well as a TESCAN MIRA 3 LMU field-emission scanning electron microscope fitted with an Oxford Instruments INCA Energy 350 X-max 80 *X*-ray analyzer (operated in backscattered electron mode).

To predict the compositions of the interaction products, thermodynamic simulation (TDS) of the metal reduction process from wolframite using aluminum and a Ca – Al master alloy was performed using the HSC Chemistry 6.12 software package. The process was simulated over a temperature range of 25–2000 °C at atmospheric pressure in a nitrogen atmosphere. To support the

simulation, the database was supplemented with missing thermodynamic data for compounds in the Al – Mn, Fe – Al, Al – Ca, Fe – W, and Al – W systems. These data were either calculated using a modified Neumann-Kopp method or taken from literature sources [26–33]. The thermodynamic properties implemented in the program are presented in **Table 1**.

The reagent consumption in thermodynamic simulation and laboratory experiments corresponded to the stoichiometry of the following reactions:

$$Mn_xFe_{1-x}WO_4 + \frac{8}{3}Al = xMn + (1-x)Fe + W + \frac{4}{3}Al_2O_3, \quad (1)$$

$$Mn_xFe_{1-x}WO_4 + \frac{20}{6}Ca_{0.6}Al_{0.4} =$$

$$= xMn + (1-x)Fe + W + 2CaO + \frac{2}{3}Al_2O_3, \quad (2)$$

where x is the atomic fraction of Mn in the compound (in unit fraction).

Results and Discussion

According to the thermodynamic simulation results **(Fig. 1)**, the temperature dependencies of the equilibrium phase composition of products from the aluminothermic reduction of wolframite were established. In the metallic phase **(Fig. 1, *a*)**, tungsten predominates, with its mass fraction increasing as temperature rises. Throughout the entire temperature range, free iron and manganese are present in the alloy, while the formation of the Fe_7W_6 and Fe_2W intermetallic compounds is possible at temperatures below 1000 °C. In the oxide phase (slag), the main component is aluminum oxide (Al_2O_3) **(Fig. 1, *b*)**. Within the temperature range of 1000-2000 °C, the $FeO{\cdot}Al_2O_3$ and $MnO{\cdot}Al_2O_3$ spinels form within the alumina matrix, with their content decreasing upon cooling. The equilibrium composition of the metallic phase at room temperature is as follows (in wt.%): 64.62 W, 13.81 Mn, 14.80 Fe_2W, 4.57 Fe_3W_6, and 2.63 Fe. Heat balance calculations demonstrated that the aluminothermic reduction of wolframite is characterized by high values of thermal effect (2598.3 kJ/kg of charge) and adiabatic temperature (3032 °C), the latter calculated without accounting for heat losses.

When using the calcium-aluminum master alloy **(Fig. 2)**, similar trends to those observed in aluminothermy are evident in the metallic phase **(Fig. 2, *a*)**: tungsten predominates, with free iron and manganese present alongside the intermetallic compounds Fe_7W_6 and Fe_2W. The distinction lies in the composition of the oxide phase **(Fig. 2, *b*)**: instead of aluminum oxide, calcium aluminates ($3CaO \cdot Al_2O_3$ and $CaO \cdot Al_2O_3$) are formed, with their content increasing as temperature rises. Minor amounts of $2CaO \cdot Al_2O_3$, $12CaO \cdot 7Al_2O_3$, as well as MnO and $MnO \cdot Al_2O_3$, are also present. The formation of low-melting calcium aluminates is expected to lower the slag melting temperature, thereby improving the conditions for separation of the metallic and slag phases. The thermal effect of wolframite reduction using the Ca – Al master alloy amounts to 2715.0 kJ/kg of charge, and the calculated adiabatic temperature (3422 °C) is 390 °C higher than that for the aluminothermic process.

Table 1
Thermodynamic properties of intermetallic compounds in the Al – Mn, Fe – Al, Al – Ca, Fe – W, and Al – W systems

Phase	Thermodynamic properties					
	ΔH_{298}, kJ/mol	S_{298}, J/(K·mol)	$C_p = A + B \cdot 10^{-3} \cdot T + C \cdot 10^5 \cdot T^{-2} + D \cdot 10^{-6} \cdot T^2$, J/(K·mol)			
			A	*B*	*C*	*D*
$Al_{12}Mn$	–114.63	340.70	419.562	–269.198	–35.171	407.348
Al_6Mn	–110.00	176.70	221.702	–78.264	–42.427	85.430
Al_4Mn	–102.25	121.63	155.796	–46.075	–28.967	56.357
$Al_{11}Mn_4$	–358.70	381.00	458.238	–91.593	–105.47	118.911
$FeAl_2$	–83.40	73.35	114.446	–81.062	–25.624	57.430
Fe_2Al_5	–213.50	161.00	193.925	–17.371	–32.081	34.052
Fe_4Al_{13}	–536.36	402.10	522.340	–169.011	–89.706	138.991
Fe_3Al	–114.57	110.12	128.594	–40.205	–69.846	29.700
FeAl	–53.40	55.55	64.849	–24.714	–23.189	20.485
$CaAl_2$	–87.84	82.00	63.860	25.381	–0.108	0.015
$CaAl_4$	–86.36	143.50	158.541	–77.958	–22.978	94.085
Ca_8Al_3	–171.93	392.23	312.539	–136.198	–15.157	407.594
Fe_2W	–8.49	87.200	80.310	–13.302	–7.337	14.415
Fe_7W_6	–42.12	392.00	380.991	–146.253	–38.792	109.161
$Al_{12}W$	–101.60	371.90	418.928	–223.080	–53.620	266.613
Al_5W	–93.20	174.00	188.110	–71.110	–31.021	81.122
Al_4W	–73.81	145.70	125.929	25.669	–12.470	11.683

Thus, the results of thermodynamic simulation demonstrated that replacing aluminum with a calcium-aluminum master alloy does not significantly affect the equilibrium composition of the metallic phase – in both cases, a W – Fe – Mn alloy with similar component contents is formed. However, the use of the Ca – Al master alloy increases the thermal effect of the process by 4.3% (from 2598.3 to 2715.0 kJ/kg of charge) and raises the adiabatic temperature by 390 °C (from 3032 to 3422 °C), which is attributed to the high exothermicity of calcium oxidation. Furthermore, the formation of low-melting calcium aluminates instead of refractory corundum is expected to provide more favorable conditions for the separation of smelting products.

Experimental verification of the thermodynamic simulation results was carried out using thermal analysis followed by XRD of the interaction products. Upon heating a mixture of wolframite with a stoichiometric amount of aluminum to 1400 °C on the DSC thermogram **(Fig. 3)**, in addition to the endothermic effect corresponding

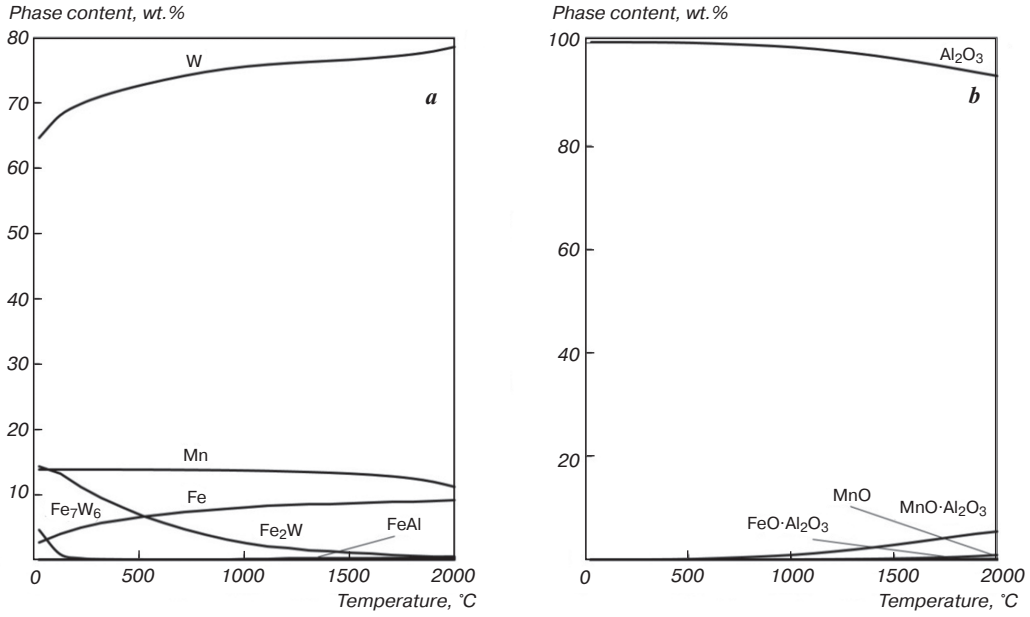

Fig. 1. Dependences of the equilibrium compositions of the products of aluminothermic reduction of wolframite on temperature: *a* – metallic phase; *b* – oxide phase

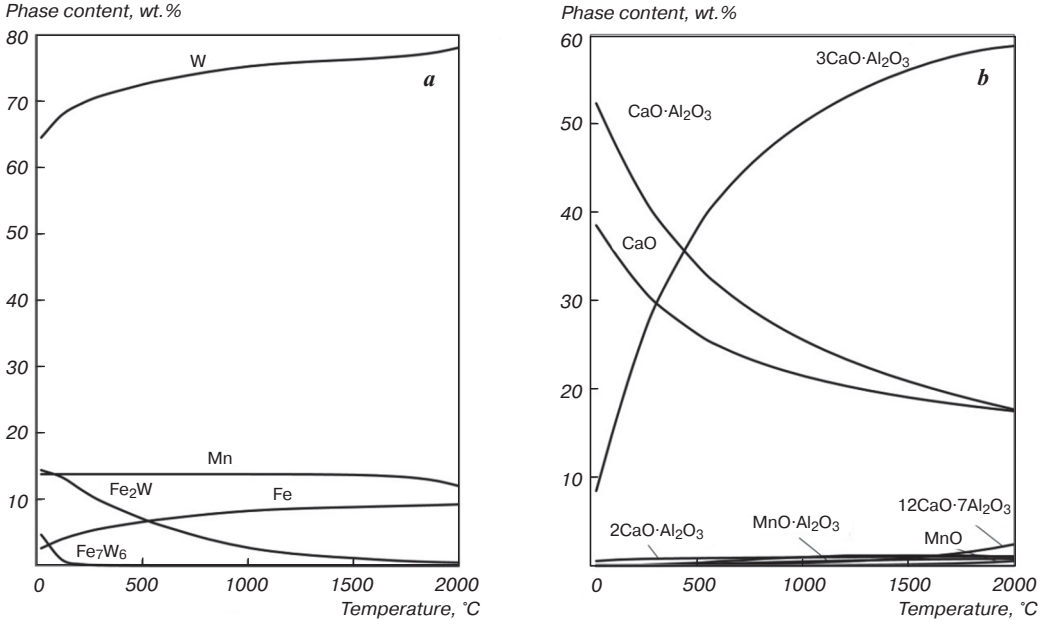

Fig. 2. Dependences of the equilibrium compositions of the products of calcium-aluminothermic reduction of wolframite on temperature: *a* – metallic phase; *b* – oxide phase

to aluminum melting, two distinct exothermic effects were observed, with onset / maximum temperatures at 893/1057 °C and 1215/1226 °C, respectively. These findings indicate a stepwise mechanism of the reduction process.

X-ray diffraction analysis of the products obtained after heating to 1200 °C revealed the formation of a metallic phase with a cubic structure characteristic of tungsten and iron (space group Im-3m, $a = 0.3161$ nm). The relatively large lattice parameter indicates a predominance of tungsten in the W_xFe_{1-x} solid solution, allowing this phase to be represented as $W_{0.95}Fe_{0.05}$ **(Table 2)**. The identified phases in the reaction products include the intermetallic compound $Mn_{11}Al_{15}$ and several oxide phases: Al_2O_3, $(Fe,Mn)Al_2O_4$, manganese tungstate Mn_3WO_6, as well as residual wolframite with unit cell parameters $a = 0.4817$ nm, $b = 0.5750$ nm, $c = 0.4994$ nm, and $= 89.01°$. Based on literature data correlating wolframite lattice parameters with the Mn/Fe ratio [34], the composition of the residual phase was determined as $Mn_{0.9}Fe_{0.1}WO_4$. These results indicate that, at the initial stage of the process, aluminum preferentially interacts with the iron-bearing components of wolframite.

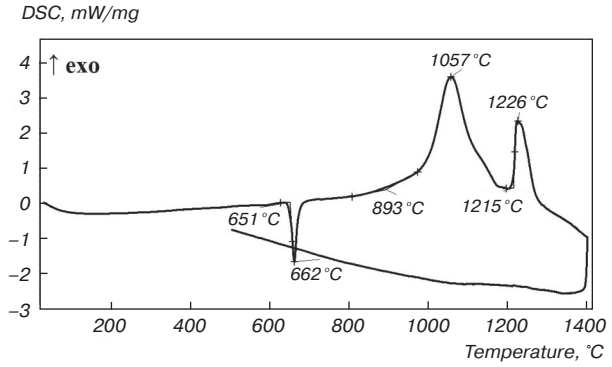

Fig. 3. DSC curve obtained during heating (upper curve) and cooling (lower curve) of a wolframite – aluminum mixture at a rate of 20 °C/min under an argon flow

Further heating to 1400-1450 °C **(Fig. 4, Table 2)** is accompanied by the completion of metal reduction from Mn_3WO_6 and $Mn_{0.9}Fe_{0.1}WO_4$ via reaction with the aluminum-based intermetallic compounds formed in the preceding stage, ultimately yielding metallic phases ($W_{0.95}Fe_{0.05}$, W_6Fe_7). No thermal effects were detected upon cooling the sample, indicating the irreversibility of the transformations that occurred.

The results of electron probe microanalysis (EPMA) of the aluminothermic reduction products obtained by heating the reagent mixture to 1450 °C at a rate of 20 °C/min are presented in **Fig. 5** and **Table 3**.

The morphology of the formed products is characterized by a fine dispersion of phases, with grain sizes ranging from 100 μm to 1-5 μm. The microstructure is heterogeneous; however, a distinct pattern is observable, consisting of light-colored grain cores rimmed by darker, fine dispersion shells. Results of local point analysis **(Table 3)** revealed that the central regions of the grains are composed of aluminum-based solid solutions of two compositions – $(Al,Fe,Mn)_5W$ and $(Al,Fe,Mn)_{12}W$ – containing up to 50 wt.% W. The high tungsten content can be attributed to the initial formation of intermetallic compounds based on Al – W [32] and Al – Mn [26], followed by their mutual dissolution. Diffusion limitations arising from insufficient process temperature hinder the

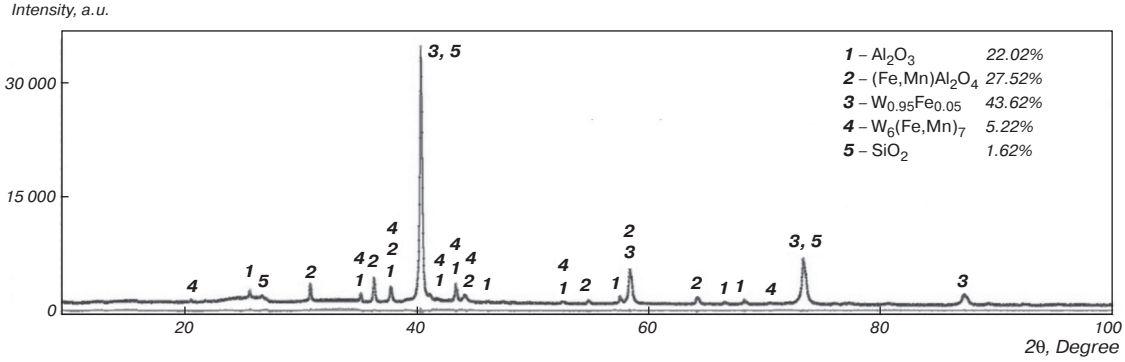

Fig. 4. *X*-ray diffraction pattern of the interaction products of wolframite with aluminum after heating to 1450 °C under an argon flow

Table 2

Charge composition and phase composition of products from aluminothermic reduction of wolframite under continuous heating conditions (20°/min)

Exp. No.	Charge composition (wt.%)		t_{max}, °C	Phase composition (Content, wt.%)	
	Wolframite	Aluminum		Metallic phase	Oxide phase
1	100	24,5	1200	$W_{0.95}Fe_{0.05}$ (32,4), $Mn_{11}Al_{15}$ (12,2)	Al_2O_3 (38,1), $(Fe,Mn)Al_2O_4$ (6,2), $Mn_{0.9}Fe_{0.1}WO_4$ (9,6), Mn_3WO_6 (1,5)
2	100	24,5	1400	$W_{0.95}Fe_{0.05}$ (43,6), $W_6(Fe,Mn)_7$ (5,2)	Al_2O_3 (22,0), $(Fe,Mn)Al_2O_4$ (27,5), SiO_2 (1,6)

complete transfer of tungsten into the reduction products. Nevertheless, a significant number of fine phases (1-5 μm in size) with a well-defined globular morphology were detected across the polished section. These phases consist of tungsten-based solid solutions with an average composition of $W_{0.95}(Al,Fe,Mn)_{0.05}$, which is consistent with the XRD data. The composition of the metallic phases is heterogeneous: in some globules, iron is absent ($W_{0.94}Al_{0.05}Mn_{0.01}$), while in others, manganese is not detected ($W_{0.96}Al_{0.03}Fe_{0.01}$). However, the compositional data for the fine grains should be considered approximate due to the inherent limitations of EPMA when applied to phases approaching the 1-5 μm size range.

The presence of globular particles, as well as compounds from the Al – Mn – Fe –W system, may be attributed to the initial formation of phases based on the Al – W system (e.g., Al_5W and $Al_{12}W$) and Fe – W [31] (e.g., Fe_7W_6), followed by their melting and subsequent compositional modification through enrichment in tungsten.

Thus, during the aluminothermic reduction of natural wolframite under continuous heating to 1450 °C, metallic phases based on tungsten with dissolved Fe, Mn, and Al are formed, alongside oxide phases predominantly composed of Al_2O_3 and $(Fe,Mn)Al_2O_4$. The reduction process proceeds in a stepwise manner and can be described by the following stages.

Initially, the process involves transformations characterized by a gradual decrease in the molar Fe/Mn ratio in wolframite from 1.0 to 0.1, driven by the reduction of Fe and W to their metallic states and the formation of tungsten aluminides. Concurrently, the formation of manganese aluminide may also occur. Based on the XRD and EPMA results, the transformations taking place during reduction can be described by the following reactions:

$$Mn_{0.5}Fe_{0.5}WO_4 + \frac{32}{27}Al = \\ = \frac{4}{9}W + \frac{4}{9}Fe + \frac{5}{9}Mn_{0.9}Fe_{0.1}WO_4 + \frac{16}{27}Al_2O_3, \quad (3)$$

$$Mn_{0.7}Fe_{0.3}WO_4 + \frac{16}{27}Al = \\ = \frac{2}{9}W + \frac{2}{9}Fe + \frac{7}{9}Mn_{0.9}Fe_{0.1}WO_4 + \frac{8}{27}Al_2O_3, \quad (4)$$

$$Mn_{0.5}Fe_{0.5}WO_4 + \frac{221}{66}Al = \\ = W + \frac{1}{2}Fe + \frac{1}{22}Mn_{11}Al_{15} + \frac{4}{3}Al_2O_3, \quad (5)$$

$$Mn_{0.7}Fe_{0.3}WO_4 + \frac{239}{66}Al = \\ = W + \frac{3}{10}Fe + \frac{7}{110}Mn_{11}Al_{15} + \frac{4}{3}Al_2O_3, \quad (6)$$

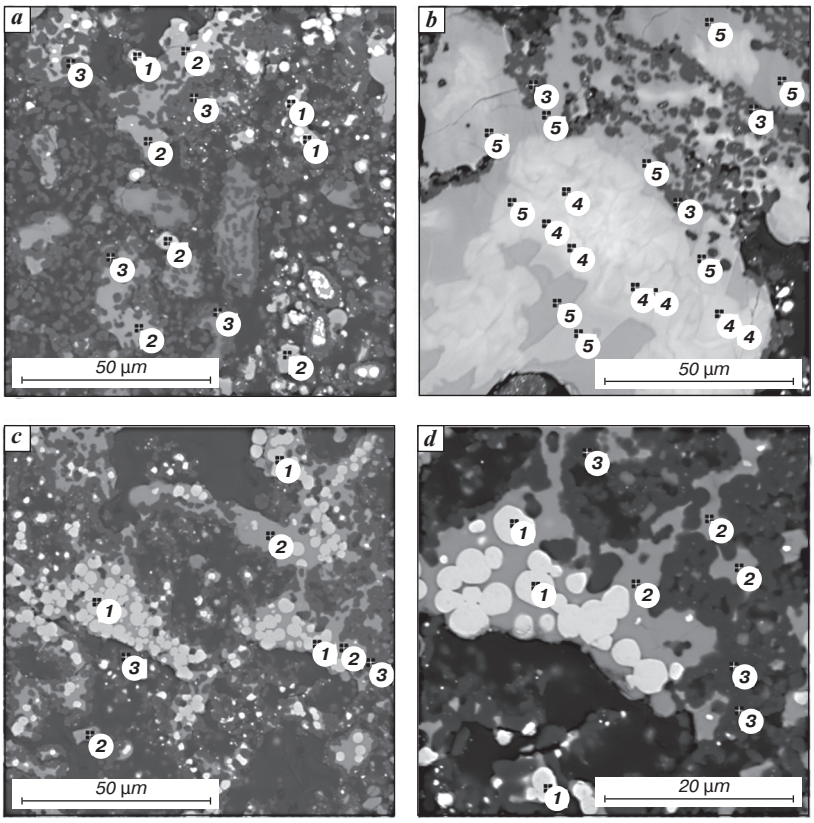

Fig. 5. Microstructure and local analysis points in the products of aluminothermic reduction of metals from wolframite, obtained after heating to 1450 °C at a rate of 20 °C/min under an argon atmosphere: (*a*, *b*, *c*) magnification ×2000 of different scanning zones; (*d*) magnification ×5000

Table 3
Phase compositions at local analysis points in the products of aluminothermic reduction of metals from wolframite, according to Fig. 5

Point No.	Content, wt.%						Presumed phase
	O	Al	P	Mn	Fe	W	
1	–	0.2–0.8	–	0.3–0.4	0–0.9	98.4–99.2	$W_{0.95}(Al,Fe,Mn)_{0.05}$
2	–	28.9–37.7	0.2–0.4	12.8–24.4	1.7–10.9	33.7–49.6	$(Al,Fe,Mn)_5W$
3	36.6–46.7	44.6–53.5	–	0.3–7.0	0.3–8.2	0–8.3	Al_2O_3
4	–	32.0–37.7	0.2–0.4	12.8–24.4	1.7–2.9	41.0–49.6	$Al_{0.68}Mn_{0.16}Fe_{0.02}W_{0.13}$
5	–	39.7–49.0	0–0.3	18.7–28.0	3.0–6.9	16.4–38.6	$(Al,Fe,Mn)_{12}W$

$$Mn_{0.5}Fe_{0.5}WO_4 + \frac{44}{3}Al = \frac{1}{2}Fe + \frac{1}{2}Mn + Al_{12}W + \frac{4}{3}Al_2O_3, \quad (7)$$

$$Mn_{0.7}Fe_{0.3}WO_4 + \frac{44}{3}Al = \frac{3}{10}Fe + \frac{7}{10}Mn + Al_{12}W + \frac{4}{3}Al_2O_3, \quad (8)$$

$$Mn_{0.5}Fe_{0.5}WO_4 + \frac{23}{3}Al = \frac{1}{2}Fe + \frac{1}{2}Mn + Al_5W + \frac{4}{3}Al_2O_3, \quad (9)$$

$$Mn_{0.7}Fe_{0.3}WO_4 + \frac{23}{3}Al = \frac{3}{10}Fe + \frac{7}{10}Mn + Al_5W + \frac{4}{3}Al_2O_3. \quad (10)$$

Subsequently, the completion of metal reduction from $Mn_{0.9}Fe_{0.1}WO_4$ occurs via interaction with manganese aluminide according to the following reactions:

$$Mn_{0.9}Fe_{0.1}WO_4 + \frac{2}{15}Mn_{11}Al_{15} = W + \frac{22}{15}Mn + (Mn_{0.9}Fe_{0.1})Al_2O_4, \quad (11)$$

$$Mn_{0.9}Fe_{0.1}WO_4 + \frac{1}{6}Al_{12}W = \frac{7}{6}W + (Mn_{0.9}Fe_{0.1})Al_2O_4, \quad (12)$$

$$Mn_{0.9}Fe_{0.1}WO_4 + \frac{2}{5}Al_5W = \frac{7}{5}W + (Mn_{0.9}Fe_{0.1})Al_2O_4. \quad (13)$$

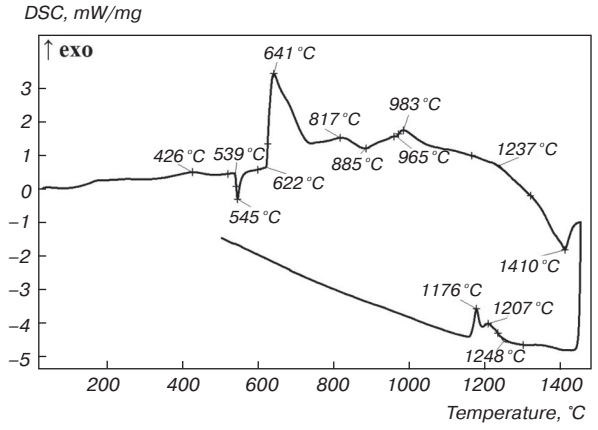

Fig. 6. DSC curve obtained during heating (upper curve) and cooling (lower curve) of a wolframite mixture with the Ca–Al master alloy at a rate of 20 °C/min under an argon flow

The interaction of wolframite with the Ca–Al master alloy (69.4% Ca) was studied using an amount of the alloy calculated to ensure complete reduction of the metals (44 wt.% relative to the mass of the mineral). According to thermal analysis data obtained by DSC, in addition to endothermic effects with onset / maximum temperatures at 540/545 °C and 1237/1410 °C – corresponding to the melting of the master alloy and oxides of the $CaO - Al_2O_3$ system, respectively – a series of exothermic effects with maxima at 641, 817, and 983 °C were detected **(Fig. 6)**. The appearance of these exothermic effects upon heating the mixture indicates the occurrence of reduction reactions. During cooling, only minor thermal effects with maxima at 1176 and 1207 °C were observed on the DSC curve, associated with a phase transition in the W – Fe-based solid solution. The absence of thermal effects in the temperature range of 500–700 °C during cooling suggests that the reducing agent was completely consumed without residue.

Upon heating a mixture of wolframite with the calcium-aluminum master alloy to 1250 °C, the reaction products were found to contain metallic phases structurally corresponding to the compounds $W_{0.7}Fe_{0.3}$ and $W_{5.14}Fe_{7.86}$, as well as an oxide component represented by calcium aluminates ($Ca_{5.65}Al_7O_{16.15}$, $Ca_3Al_2O_6$, and $CaAl_2O_4$) **(Table 4)**. The lattice parameter of the $W_{0.7}Fe_{0.3}$ phase (a = 0.3161 nm) is close to that of the product obtained via aluminum reduction; therefore, it is appropriate to represent the formula of this compound as $W_{0.95}Fe_{0.05}$.

The primary distinction between calcium-aluminothermic reduction and conventional aluminothermy lies in the complete absence of residual wolframite (of the $Mn_{0.9}Fe_{0.1}WO_4$ type), accompanied by the simultaneous formation of $CaWO_4$, Ca_3WO_6, Ca_2WMnO_6, and $W_{0.5}Fe_{0.5}O_{0.5}$. The appearance of the latter phase is attributed to the incomplete reduction of tungsten oxides during the initial stage, resulting from diffusion limitations imposed by the formation of mayenite ($Ca_6Al_7O_{16}$), whose melting point exceeds the investigated temperature range (up to 1250 °C). The formation of calcium-containing tungstates with varying stoichiometries indicates a fundamentally different reaction mechanism compared to aluminothermy. At the initial stage, the process can be described by the following principal reaction equations

Table 4
Charge composition and phase composition of products from calcium-aluminothermic reduction of wolframite under continuous heating conditions (20 °C/min)

Exp. No.	Charge composition (wt.%)		t_{max}, °C	Phase composition (Content, wt.%)	
	Wolframite	Ca – Al Master Alloy		Metallic phase	Oxide phase
1	100	44,0	1250	$W_{0.95}Fe_{0.05}$ (45,2), $W_{5.15}(Fe,Mn)_{7.86}$ (11,0)	$Ca_{5.65}Al_7O_{16.15}$ (25,3), $Ca_3Al_2O_6$ (3,8), CaO (3,8), $CaWO_4$ (2,4), $CaAl_2O_4$ (1,5), $W_{0.5}Fe_{0.5}O_{0.5}$ (2,0), Ca_3WO_6 (1,7), Ca_2WMnO_6 (1,7)
2	100	44,0	1450	W (16,7), $W_6(Fe,Mn)_7$ (7,5)	$Ca_{12}Al_{14}O_{33}$ (53,2), SiO_2 (4,8), $CaAl_2O_4$ (14,3), Al_2O_3 (3,5)

(the chemical composition of the master alloy is represented as $Ca_{0.6}Al_{0.4}$):

$$Mn_{0.5}Fe_{0.5}WO_4 + \frac{35}{17}Ca_{0.6}Al_{0.4} = \\ = \frac{8}{17}W + \frac{1}{2}Fe + \frac{1}{2}Mn + \frac{9}{17}CaWO_4 + \frac{2}{17}Ca_6Al_7O_{16}, \quad (14)$$

$$Mn_{0.7}Fe_{0.3}WO_4 + \frac{35}{17}Ca_{0.6}Al_{0.4} = \\ = \frac{8}{17}W + \frac{3}{10}Fe + \frac{7}{10}Mn + \frac{9}{17}CaWO_4 + \frac{2}{17}Ca_6Al_7O_{16}, \quad (15)$$

$$Mn_{0.5}Fe_{0.5}WO_4 + \frac{14}{5}Ca_{0.6}Al_{0.4} = \\ = \frac{19}{25}W + \frac{1}{2}Fe + \frac{1}{2}Mn + \frac{6}{25}Ca_3WO_6 + \frac{4}{25}Ca_6Al_7O_{16}, \quad (16)$$

$$Mn_{0.7}Fe_{0.3}WO_4 + \frac{14}{5}Ca_{0.6}Al_{0.4} = \\ = \frac{19}{25}W + \frac{3}{10}Fe + \frac{7}{10}Mn + \frac{6}{25}Ca_3WO_6 + \frac{4}{25}Ca_6Al_7O_{16}, \quad (17)$$

$$Mn_{0.5}Fe_{0.5}WO_4 + \frac{140}{59}Ca_{0.6}Al_{0.4} = \\ \frac{41}{59}W + \frac{1}{2}Fe + \frac{23}{118}Mn + \frac{18}{59}Ca_2MnWO_6 + \frac{8}{59}Ca_6Al_7O_{16}, \quad (18)$$

$$Mn_{0.7}Fe_{0.3}WO_4 + \frac{140}{59}Ca_{0.6}Al_{0.4} = \\ = \frac{41}{59}W + \frac{3}{10}Fe + \frac{233}{590}Mn + \\ + \frac{18}{59}Ca_2MnWO_6 + \frac{8}{59}Ca_6Al_7O_{16}. \quad (19)$$

The results of electron probe microanalysis (EPMA) of the interaction products between wolframite and the Ca – Al master alloy after heating to 1250 °C **(Fig. 7, Table 5)** revealed a fine dispersion and considerable diversity of the formed phases. A zonal distribution within the particles was identified: the outer regions are covered by oxide phases, while the interiors consist of fine metallic grains (~1–2 μm in size). In some particles, alternating oxide and metallic zones were observed. The metallic phases are predominantly composed of solid solutions based on $W_{5.14}(Fe,Mn)_{7.86}$, $(Fe,Mn)_7W_6$, and $W_{0.95}(Al,Fe,Mn)_{0.05}$, which is consistent with the XRD data. The manganese content in the ferrotungsten metallic grains varies within the range of 1.1-9.7 wt.%. Additionally, fragments of metallic phases corresponding to MnAl were detected across the polished section. The oxide phases are represented by calcium aluminates ($Ca_{5.65}Al_7O_{16.15}$), calcium tungstates ($CaWO_4$, Ca_3WO_6), aluminum oxide (Al_2O_3), and solid solutions of the $(CaO - WO_3 - MnO)_{ss}$ type. Nearly all oxide phases, with the exception of calcium aluminates, contain both tungsten and manganese.

Further heating to 1450 °C promotes the completion of tungsten reduction, resulting in its accumulation in elemental form and as $W_6(Fe,Mn)_7$. The reducing agents are most likely the MnAl intermetallic compound identified by EPMA **(Table 5)**, along with calcium, which exists as vapor within this temperature range (1250-1450 °C) and is consequently undetected in the cooled product by XRD and EPMA. The absence of tungsten-containing compounds in the oxide phase **(Fig. 8, Table 4)** confirms that the reduction of tungsten by the Ca – Al master alloy is complete under the high-temperature experimental conditions.

The reaction scheme above 1250 °C can be represented by the following principal equations:

$$CaWO_4 + 2MnAl = W + 2Mn + CaAl_2O_4, \quad (20)$$

$$Ca_3WO_6 + 2MnAl = W + 2Mn + \frac{1}{7}Ca_{12}Al_{14}O_{33} + \frac{9}{7}CaO, \quad (21)$$

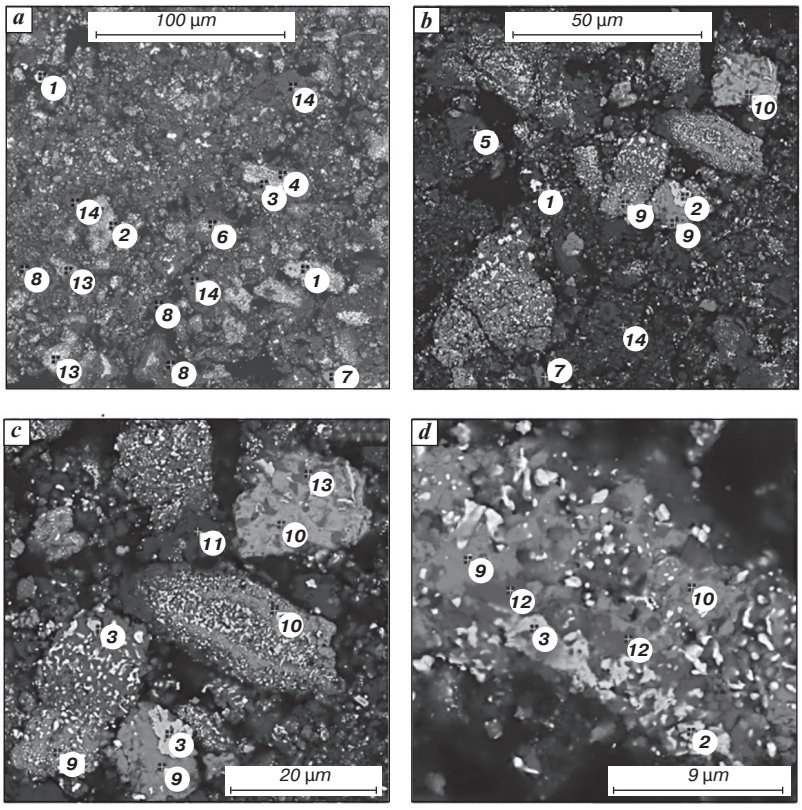

Fig. 7. Microstructure and local analysis points in the products of metal reduction from wolframite using the Ca – Al master alloy, obtained after heating to 1250 °C at a rate of 20 °C/min under an argon atmosphere: (*a*) magnification ×1000; (*b*) ×2000; (*c*) ×4000; (*d*) ×10000

$$Ca_2WMnO_6 + \frac{8}{3}MnAl = = W + \frac{11}{3}Mn + \frac{1}{6}Ca_{12}Al_{14}O_{33} + \frac{1}{6}Al_2O_3, \quad (22)$$

$$CaWO_4 + 3Ca_{vap} = W + 4CaO, \quad (23)$$

$$Ca_3WO_6 + 3Ca_{vap} = W + 2CaO, \quad (24)$$

$$Ca_2WMnO_6 + 4Ca_{vap} = W + Mn + 6CaO, \quad (25)$$

$$Al_2O_3 + \frac{12}{7}CaO = \frac{1}{7}Ca_{12}Al_{14}O_{33}, \quad (26)$$

$$Al_2O_3 + CaO = CaAl_2O_4. \quad (27)$$

As noted above, in the aluminothermic process, the slag phase consists predominantly of corundum (Al_2O_3, m.p. = 2050 °C), which is characterized by high viscosity even in the superheated state, complicating the "metal–slag" gravitational separation and increasing the mechanical losses of tungsten. The addition of fluxing additives (CaO, CaF_2) allows for a reduction in the liquidus temperature and melt viscosity due to the formation of low-melting eutectics and aluminates; however, it leads to charge dilution and a decrease in the specific productivity of the process. The use of a Ca – Al master alloy solves this problem by combining the functions of a reducing agent and a source of the fluxing component (CaO). As shown in [23], the oxidation of calcium from the master alloy is accompanied by the formation of mayenite-like phases (e.g., $Ca_{12}Al_{14}O_{33}$, m.p. = 1455 °C), which, at the operating temperatures of the process, provide favorable rheological conditions for the separation of the smelting products.

Thus, the conducted studies have revealed a fundamental difference in the mechanism of wolframite interaction with a simple versus a complex reducing agent. When aluminum is used, the process proceeds in a stepwise manner: initially, aluminum interacts with the

Table 5

Phase compositions at local analysis points in the products of metal reduction from wolframite using a Ca – Al master alloy, according to Fig. 7

Point No.	Content, wt.%						Average phase composition
	O	Al	Ca	Mn	Fe	W	
1	–	0.7–1.1	–	0.6–0.7	–	97.5–98.7	$W_{0.95}(Al,Fe,Mn)_{0.05}$
2	–	–	1.4–3.4	6.0–9.7	22.3–24.7	64.3–67.7	$W_{5.14}(Fe,Mn)_{7.86}$
3	–	–	0.4–0.9	1.1–7.1	22.4–25.8	70.5–76.1	$(Fe,Mn)_7W_6$
4	–	1.6	–	1.9	6.44	90.0	$W_{0.7}(Fe,Mn)_{0.3}$
5	46.7	25.2	28.1	–	–	–	$CaAl_2O_4$
6	–	–	4.9	45.1	10.2	39.8	$W_{13}(Fe,Mn)_{74}$
7	–	26.1–36.4	0.3–0.5	53.7–64.4	1.4–3.2	6.0–8.1	MnAl
8	37.0–40.1	55.9–57.2	0.3–5.9	–	–	–	Al_2O_3
9	15.5–19.9	–	19.9–27.6	3.9–6.0	–	49.7–59.6	Ca_3WO_6
10	13.7–22.4	–	11.4–14.1	1.7–5.9	0.7	62.6–68.3	$CaWO_4$
11	27.9–34.8	1.2–1.5	43.8–52.4	1.8–4.8	1.1–1.2	9.1–17.0	$(CaO – Ca_3WO_6)_{ss}$
12	20.7–25.1	–	25.7–28.9	40.5–44.7	1.9	5.7–8.1	$(MnO – CaO)_{ss}$
13	18.8–26.6	0.4	6.3–12.3	34.5–42.2	1.3–2.6	27.2–32.6	$(MnO – WO_3 – CaO)_{ss}$
14	38.2–46.7	25.2–26.8	28.1–31.5	1.2	–	2.4–3.7	$Ca_{5.65}Al_7O_{16.15}$

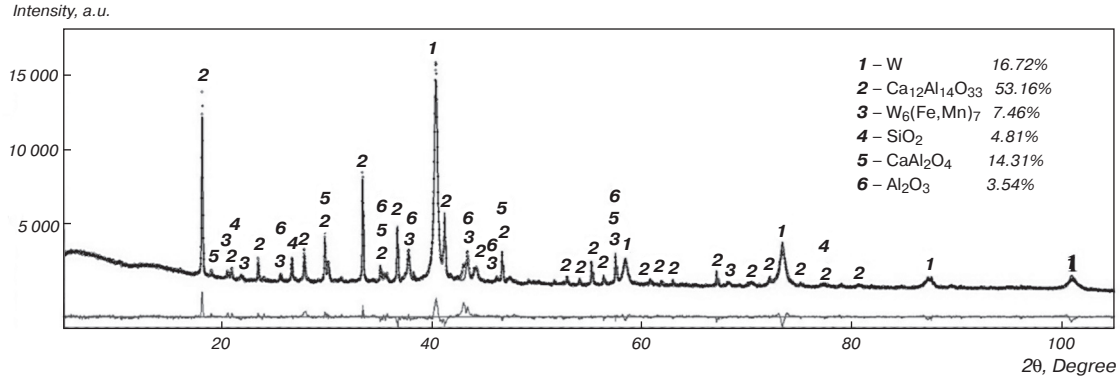

Fig. 8. *X*-ray diffraction pattern of the interaction products of wolframite with the Ca – Al master alloy after heating to 1450 °C under an argon flow

iron-bearing phase of wolframite, leading to the formation of aluminides of the principal metals and residual wolframite enriched in manganese; subsequently, the metal aluminides reduce the residual wolframite. In the case of the Ca – Al master alloy, calcium tungstates of varying stoichiometry and manganese aluminides are formed at the initial stages; together with calcium vapor, they sequentially reduce the calcium-containing tungstates. Regardless of the type of reducing agent, the final metallic phases are metallic tungsten and its solid solutions with Fe and Mn ($W_{0.95}Fe_{0.05}$ and $W_6(Fe,Mn)_7$), which is consistent with the results of thermodynamic simulation. A distinctive feature of the calcium-aluminothermic process is the formation of calcium aluminates with a mayenite-type structure, which transition to a molten state at temperatures above 1450 °C and facilitate contact between the reducing agent and the residual oxide component.

Conclusions

Regardless of the type of reducing agent employed (Al or Ca – Al master alloy), the metallothermic reduction of wolframite yields products of similar composition, containing metallic tungsten and ferrotungsten. The advantage of using the Ca – Al master alloy lies in the higher thermal effect of the reduction process (2715.0 kJ/kg versus 2598.3 kJ/kg for Al) and, consequently, in an increase of the adiabatic temperature by 390 °C, which is attributed to the high exothermicity of the calcium oxidation reaction.

The stepwise nature of the aluminothermic reduction of wolframite has been experimentally confirmed. Up to a temperature of 1200 °C, aluminum reacts with the iron-bearing components of the mineral, forming aluminides structurally corresponding to $Mn_{11}Al_{15}$, $Al_{12}W$, and Al_5W, alongside a manganese-enriched residual wolframite ($Mn_{0.9}Fe_{0.1}WO_4$). Increasing the temperature to 1450 °C initiates the reduction of the residual oxide phase by the formed tungsten and manganese aluminides, yielding $W_{0.95}Fe_{0.05}$ and $W_6(Fe,Mn)_7$ alloys.

The application of a Ca – Al master alloy (69.4 wt.% Ca) fundamentally alters the reaction mechanism: at the initial stage, calcium tungstates of varying stoichiometry ($CaWO_4$, Ca_3WO_6, and Ca_2WMnO_6) are formed, along with manganese aluminide. Upon heating above 1450 °C, MnAl, in conjunction with calcium vapor, ensures the complete reduction of calcium-containing tungstates to metallic tungsten and $W_6(Fe,Mn)_7$. When the Ca – Al master alloy is used, the oxide phase consists predominantly of low-melting calcium aluminates, which, unlike the refractory corundum formed in aluminothermy, create more favorable conditions for separation of slag and metal.

Regardless of the type of reducing agent employed, the interaction of wolframite with either aluminum or a Ca – Al master alloy culminates in the formation of a metallic product consisting of tungsten and its solid solutions with iron and manganese. This conclusion is supported by the consistent results obtained from both experiments and thermodynamic simulation.

The work was carried out according to the State Assignment for the Vatolin Institute of Metallurgy of the Ural Branch of the Russian Academy of Sciences (IMET UB RAS) using the equipment of the Collaborative Usage Center "Ural-M".

References

1. Jiang D., Zhong S., Xiao W., et al. Structural, Mechanical, Electronic, and Thermodynamic Properties of Pure Tungsten Metal Under Different Pressures: a First-Principles Study. *International Journal of Quantum Chemistry*. 2020. Vol. 120, Iss. 13. e26231.

2. Zhao J., Jiang Z. Development of New Microalloyed Steel by Alloying with Tungsten. *Applied Mechanics and Materials*. 2015. Vols. 716–717. pp. 48–51.

3. Ravi Kiran U., Panchal A., Prem Kumar M., et al. Refractory Metal Alloying: a New Method for Improving Mechanical Properties of Tungsten Heavy Alloys. *Journal of Alloys and Compounds*. 2017. Vol. 714. pp. 1035–1044.

4. Rozhikhina I. D., Nokhrina O. I., Yolkin K. S., et al. Ferroalloy Production: State and Development Trends in the World and Russia. *IOP Conference Series: Materials Science and Engineering*. 2020. Vol. 866. 012004.

5. Zinyagin A. G., Borisenko N. R., Stepanov A. P., Kryuchkova M. O. Development of Measures to Reduce Longitudinal Bending of Thick Clad and Alloyed Steel Plates During Hot Rolling. *CIS Iron and Steel Review*. 2025. Vol. 29. pp. 56–60.

6. Gorbatyuk S. M., Pavlov V. M., Shapoval A. N., Gorbatyuk M. S. Experimental Use of Rotary Rolling Mills to Deform Compacts of Refractory Metals. *Metallurgist*. 1998. Vol. 42, Iss. 5. pp. 178–183.

7. Venables D. S., Brown M. E. Reduction of Tungsten Oxides with Carbon. Part 1: Thermal Analyses. *Thermochimica Acta*. 1996. Vols. 282–283. pp. 251–264.

8. Zayko V. P., Zhuchkov V. I., Drobyshevsky P. A., et al. Technology of Tungsten-Containing Ferroalloys. Ekaterinburg: Ural Branch of the Russian Academy of Sciences, 2005. 557 p.

9. Yucel O., Ozcelebi M. A. Reduction Smelting of Bursa-Uludag Tungsten Concentrates by the Aluminothermic Process. *Scandinavian Journal of Metallurgy*. 2000. Vol. 29, Iss. 3. pp. 108–113.

10. Golovchenko N., Bairakova O., Aknazarov S., et al. Extraction of Ferrotungsten from Ores with Low WO_3 Content. *International Journal of Self-Propagating High-Temperature Synthesis*. 2012. Vol. 21, Iss. 3. pp. 156–161.

11. Khatkov V. Yu., Boyarko G. Yu. Current State of Tungsten Industry in Russia. *Bulletin of the Tomsk Polytechnic University. Geo Assets Engineering*. 2019. Vol. 330, Iss. 2. pp. 124–137.

12. Yang X. Beneficiation Studies of Tungsten Ores – a Review. *Minerals Engineering*. 2018. Vol. 125. pp. 111–119.

13. Kolosov V. N., Miroshnichenko M. N., Prokhorova T. Yu. Investigation of the Preparation of W-Cr System Powders from Oxide Compounds by Magnesium Vapors Reduction. *Journal of Physics: Conference Series*. 2021. Vol. 1758. 012017.

14. Ricceri R., Matteazzi P. A Study of Formation of Nanometric W by Room Temperature Mechanosynthesis. *Journal of Alloys and Compounds*. 2003. Vol. 358, Iss. 1–2. pp. 71–75.

15. Yang X., Tan D.-Q., Li Y.-L., et al. The Influence of Calcium Additive in the Structural Formation of Tungsten Via Reduction Reaction. *Advanced Materials Research*. 2015. Vol. 1088. pp. 159–163.

16. He W., Tan D., Kuang H., et al. A systematic Study of the Effect of Calcium on the Production and Properties of WC Precursor Powders and Alloys. *International Journal of Refractory Metals and Hard Materials*. 2018. Vol. 84. pp. 140–148.

17. Chang H.-Q., Zhang G.-H. A Novel Green Strategy for the Preparation of Ultrafine-Grained WSi_2 and W_5Si_3 Powders. *Ceramics International*. 2022. Vol. 48, Iss. 21. pp. 31880–31889.

18. Pashkeev K. Yu., Pashkeev I. Yu., Mikhailov G. G., Sudarikov M. V., Tarasov P. A. Research of Aluminothermic Reduction of Wolframite Concentrates. *Bulletin of the South Ural State University. Ser. Metallurgy*. 2015. Vol. 15, Iss. 2. pp. 13–19.

19. Golovchenko N. Yu., Bairakova O. S., Ksandopulo G. I., et al. Reception of Ferrotungsten from Wolframite Concentrate by Aluminothermic Method. *Eurasian Chemico-Technological Journal*. 2011. Vol. 13, Iss. 3-4. pp. 205–212.

20. Wang Y., Jiang W., Cheng Z., et al. Thermite Reactions of Al/Cu Core-Shell Nanocomposites with WO_3. *Thermochimica Acta*. 2007. Vol. 463, Iss. 1–2. pp. 69–76.

21. Sakaki M., Bafghi M. Sh., Vahdati Khaki J., et al. Effect of the Aluminum Content on the Behavior of Mechanochemical Reactions in the WO_3–C–Al System. *Journal of Alloys and Compounds*. 2009. Vol. 480, Iss. 2. pp. 824–829.

22. Gorkunov V., Munter R. Calcium-Aluminothermal Production of Niobium and Mineral Composition of the Slag. *Proceedings of the Estonian Academy of Sciences. Chemistry*. 2007. Vol. 56, Iss. 3. pp. 142–156.

23. Pikulin K. V., Tyushnyakov S. N., Gulyaeva R. I., et al. Phase Formation Features in the Metallothermal Reduction of Natural Coltan. *Metals*. 2026. Vol. 16, Iss. 4. 436.

24. Gulyaeva R. I., Udoeva L. Yu., Petrova S. A., et al. Phase Transformation During Metallothermic Reduction of Tantalite. *Metallurgist*. 2022. Vol. 66, Iss. 1–2. pp. 200–214.

25. Selivanov E. N., Pikulin K. V., Galkova L. I., et al. Kinetics and Mechanism of Natural Wolframite Interactions with Sodium Carbonate. *International Journal of Minerals, Metallurgy and Materials*. 2019. Vol. 26, Iss. 11. pp. 1364–1371.

26. Shukla A., Pelton A. D. Thermodynamic Assessment of the Al – Mn and Mg – Al – Mn Systems. *Journal of Phase Equilibria and Diffusion*. 2009. Vol. 30, Iss. 1. pp. 28–39.

27. Gasior W., Debski A., Moser Z. Formation Enthalpy of Intermetallic Phases from Al-Fe System Measured with Solution Calorimetric Method. *Intermetallics*. 2012. Vol. 24. pp. 99–105.

28. Islam F., Medraj M. Thermodynamic Modeling of Mg – Ca and Al – Ca Binary Systems. *CSME 2004 Forum*. 2004. pp. 921–929.

29. Ozturk K., Chen L.-Q., Liu Z.-K. Thermodynamic Assessment of the Al – Ca Binary System Using Random Solution and Associate Models. *Journal of Alloys and Compounds*. 2002. Vol. 340, Iss. 1–2. pp. 199–206.

30. Merlo F. Heat Capacities from 400 to 1200 K of $CaAl_2$, $EuAl_2$, $ErAl_2$ and of the Intermediate Valence Compound $YbAl_2$. *Thermochimica Acta*. 1983. Vol. 64, Iss. 1-2. pp. 115–122.

31. Jacob A., Schmetterer C., Singheiser L., et al. Modeling of Fe–W Phase Diagram Using First Principles and Phonons Calculations. *CALPHAD: Computer Coupling of Phase Diagrams and Thermochemistry*. 2015. Vol. 50. pp. 92–104.

32. Wang C., Liang S., Cui J., et al. First-Principles Study of the Mechanical and Thermodynamic Properties of Al_4W, Al_5W and $Al_{12}W$ Under Pressure. *Vacuum*. 2019. Vol. 169. 108844.

33. Joubert J.-M., Kaplan B., Selleby M. The Specific Heat of Al-based Compounds, Evaluation of the Neumann-Kopp rule and Proposal for a Modified Neumann-Kopp Rule. *CALPHAD: Computer Coupling of Phase Diagrams and Thermochemistry*. 2023. Vol. 81. 102562.

34. Sint O., Min M. M. Structural, Electrical and Magnetic Properties of Wolframite ($FeMnWO_4$) from Pharchaung Mine in Tanintharyi Region. *Journal of the Myanmar Academy of Arts and Science*. 2018. Vol. 16, Iss. 2. pp. 139–148.

NFM